



HHS Public Access

Author manuscript

Bioorg Med Chem Lett. Author manuscript; available in PMC 2019 September 01.

Published in final edited form as:

Bioorg Med Chem Lett. 2018 September 01; 28(16): 2741–2745. doi:10.1016/j.bmcl.2018.02.040.

A Chemically Stable Fluorescent Marker of the Ureter

Jaepyeong Cha^{a,*}, Roger R. Nani^b, Michael P. Luciano^b, Aline Broch^a, Kihoon Kim^{a,c}, Jung-Man Namgoong^{a,d}, Rhushikesh A. Kulkarni^b, Jordan L. Meier^b, Peter Kim^a, and Martin J. Schnermann^{b,*}

^aSheikh Zayed Institute for Pediatric Surgical Innovation, Children's National Health System, 111 Michigan Ave. NW Washington, DC 20010, United States

^bChemical Biology Laboratory, Center for Cancer Research, National Cancer Institute, Frederick, Maryland 21702, United States

^cDepartment of Surgery, Inje University Haeundae Paik Hospital, 875 Haeun-daero, Haeundaegu, Busan 612-896, South Korea

^dDepartment of Surgery, Asan Medical Center, 88 Olympic-ro 43-gil, Songpa-gu, Seoul 138-736, South Korea

Abstract

Surgical methods guided by exogenous fluorescent markers have the potential to define tissue types in real time. Small molecule dyes with efficient and selective renal clearance could enable visualization of the ureter during surgical procedures involving the abdomen and pelvis. These studies report the design and synthesis of a water soluble, net neutral C4'-*O*-alkyl heptamethine cyanine, Ureter-Label (UL)-766, with excellent properties for ureter visualization. This compound is accessed through a concise synthetic sequence involving an *N*- to *O*- transposition reaction that provides other inaccessible C4'-*O*-alkyl heptamethine cyanines. Unlike molecules containing a C4'-*O*-aryl substituent, which have also been used for ureter visualization, UL-766 is not reactive towards glutathione and the cellular proteome. In addition, rat models of abdominal surgery reveal that UL-766 undergoes efficient and nearly exclusive renal clearance *in vivo*. In total, this molecule represents a promising candidate for visualization of the ureter during a variety of surgical interventions.

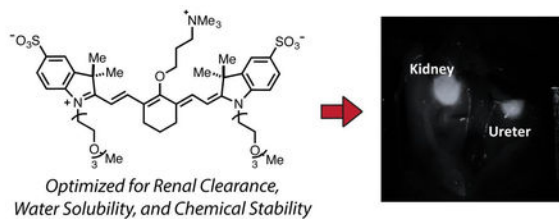
Graphical Abstract

*Corresponding authors: JCHA2@childrensnational.org (J. Cha.), martin.schnermann@nih.gov (M. Schnermann).

Publisher's Disclaimer: This is a PDF file of an unedited manuscript that has been accepted for publication. As a service to our customers we are providing this early version of the manuscript. The manuscript will undergo copyediting, typesetting, and review of the resulting proof before it is published in its final citable form. Please note that during the production process errors may be discovered which could affect the content, and all legal disclaimers that apply to the journal pertain.

A. Supplementary data

Supplementary data associated with this article can be found, in the online version, at <https://doi.org/10.1016/j.bmcl.2018.02.040>.



Keywords

Fluorophore synthesis; Near-IR fluorescence; Fluorescence-Guided Surgery

Despite remarkable progress in molecular medicine, surgical interventions are nearly always carried out using only visual, memory recall, and tactile cues. Adding insight through imaging is being explored with diverse modalities.¹ Fluorescence-guided surgical (FGS) methods provide real-time images using only relatively simple optical readouts.^{2,3} These methods are progressing toward clinical use in a variety of disease contexts.⁴ Fluorescent dyes, ideally with emission in the near-infrared (NIR) range (~700-900 nm), form the chemical component of these efforts.^{3,5,6} Most clinical efforts use indocyanine green (ICG), which was FDA approved nearly 60 years ago.⁷ To enable the broad adaptation of FGS, a new generation of dyes that address specific challenges in the field are needed.

The identification and precise dissection of critical structures is central to the surgical process. Unintended injury results in short and long-term complications, prolonged hospital stays and health care costs. Acute ureteral injury results from external trauma, open surgery, laparoscopy and endoscopic procedures. Nearly any abdominopelvic surgical procedure, whether gynecologic, obstetric, general surgical, or urologic can potentially injure the ureter. The incidence of ureter injury during abdominal and pelvic surgery has been reported to range from 0.5% to 10%.⁶⁻⁸ An analysis of 13 studies concluded that the following procedures contribute to iatrogenic ureteral injuries: hysterectomy (54%), colorectal surgery (14%), pelvic procedures such as ovarian tumor removal (8%), transabdominal urethropexy (8%), and abdominal vascular surgery (6%).⁹ The total incidence of ureteral injury after gynecologic surgery is reported to be 0.5% to 1.5%, and after abdominoperineal colon resection ranges from 0.3% to 5.7%.⁹ The ureter is vulnerable to iatrogenic injuries because of its close proximity to vital visceral organs and its 'hidden location' in the retroperitoneum of the abdomen and pelvis. Clear visualization during surgery through FGS could alleviate this significant morbidity. Prior work, including clinical trials, has centered on using methylene blue to illuminate the ureter during surgery.^{8,9} However, this molecule does not absorb/emit in the NIR range, where light can maximally penetrate tissue, and also exhibits equal amounts of hepatic clearance. One study has reported the use of IR800-CW, though as described below, we observe significant competitive hepatic clearance rendering this molecule suboptimal for use in this context.¹⁰ In these studies, we report the design, synthesis, and application of a novel net-neutral near-IR dye, which we term (Ureter-Label (UL)-766), that exhibits excellent chemical stability, is readily synthesized, and rapidly cleared through renal pathways. These characteristics make this compound an excellent candidate for use as a ureter marker in FGS.

The design of UL-766 was informed by several insights. Heptamethine cyanines are privileged molecules for *in vivo* optical imaging, with absorbance and emission maxima around 800 nm. Modifying substituents of the core cyanine scaffold provides a useful means to tune its biological properties.^{11–14} We recently reported a novel group of cyanine fluorophores, exemplified by FNIR-774 (Figure 1).¹⁵ Synthetic access is enabled by an *N*- to *O*-rearrangement reaction sequence, providing a general approach to prepare otherwise inaccessible C4'-*O*-alkyl heptamethine cyanines.^{15–18} Several prior studies examined the effect of cyanine polarity and functionality on biodistribution and clearance. In particular, Choi and others have shown that the attachment of polar functional groups, specifically quarternized trimethylalkylammoniums, can dramatically alter clearance pathways.^{19–21} The resulting fluorophores, often as targeted conjugates, exhibit useful *in vivo* targeting and efficient renal clearance. While useful, these molecules contain phenols at the C4'-position, which may render them subject to covalent modification (see below).¹⁵

These studies report the discovery and characterization of UL-766. This molecule has triethylene glycol chains appended to the two indolenine nitrogens. This substituent, in combination with the aryl sulfonates, was anticipated to provide excellent water solubility. Our prior studies have suggested that installing a charged functional group proximate to the C4'-position of cyanine polyene serves to mitigate the formation of undesirable H-aggregates, a common issue with these molecules.^{15, 22, 23} To introduce this charge, as well as to provide net-neutral molecules, we installed a trimethylalkyl-ammonium ether at the C4' position. To examine the role of the alkyl linker, we have prepared both propyl and ethyl variants.

The synthesis of cyanines **8** and **9** is outlined in Scheme 1. The sequence commenced with alkylation of indolenine **1** with iodide **2** in MeCN at 120 °C to provide **3** in 45% yield. Conventional cyanine formation with **3** and commercial **4** in refluxing EtOH with Et₃N and Ac₂O affords **5** in 46% yield following reversed-phase purification. The ethyl congener could be accessed through a two-step sequence starting with *N*-methylethanol amine addition in DMF at 75 °C to afford **6** in 85% yield. The Smiles-type rearrangement of **6** proceeds as reported previously on a similar substrate using MeI, NaHCO₃ in DMF at 95 °C to provide **8** in 86% yield.¹⁵ To access the propyl variant, we first prepared **7** through *N*-methylpropanolamine addition to **5** in DMF at 100 °C in 74% yield. While direct rearrangement of **7** with the MeI, NaHCO₃ in DMF conditions was ineffective, we found that TFA treatment, solvent removal, followed by heating with excess MeI and NaHCO₃ in DMF provided **9** in 67% yield from **7**. In this instance, TFA treatment of **7** induces an *N*- to *O*-transposition (based on a bathochromic shift in the absorbance maxima), which then undergoes *N*-alkylation. Of note, the latter sequence has been applied on 0.5 g scale, which has provided sufficient material for extensive *in vivo* testing.

We investigated the spectroscopic properties of compounds **8** and **9**. As anticipated, these molecules have similar properties to related heptamethine cyanines, such as FNIR-774 (Table 1). Moreover, **8** and **9** display excellent water solubility of up to 5 mM in pH 7.4 PBS.

We have examined the thiol reactivity of these molecules. These studies build on the prior observation that FNIR-774 (a C4'-O-alkyl cyanine) is nearly immune to the thiol-substitution reactions (Figure 2A), while C4'-phenol-substituted variants undergo thiol-exchange readily.^{15, 24, 25} We first compared the reactivity of **8**, **9** and IRDye-800CW in 1 mM glutathione (GSH) in pH 7.4 PBS using an HPLC assay (Figure 2B). These conditions are identical to our prior efforts where we found that FNIR-774 was not subject to thiol addition.¹⁵ We observed that IRDye-800CW is consumed with an approximate half-life ($t_{1/2}$) of 2 h with clean formation of the resulting GSH adduct, which could be observed by mass spectral analysis. Somewhat to our surprise, and unlike with our prior C4'-alkyl ether cyanines, the ethyl linker variant **8** is subject to the same reaction, albeit with moderately slower kinetics compared to IRDye-800CW under identical conditions. Gratifyingly, we found that compound **9**, which has a propyl linker to the trimethyl-ammonium functional group, was unreactive in these conditions, with >95% of the starting material surviving after 12 h incubation at rt. This result suggests that C4'-O-alkyl cyanines can undergo thiol exchanges in cases where strong-electron withdrawing functional groups are appended to the β -, but apparently not the γ -, position.

We then examined the possibility that this thiol-substitution reaction might also occur in a proteomic context. Whole-cell lysate, obtained from HEK-293 cells, was incubated with **8**, **9**, FNIR-774, and IRDye-800CW for 24 h at rt. The respective mixtures were then run on an SDS-PAGE gel and gel bands were visualized on the 800 nm emission channel. This approach allows for the visualization of proteins modified covalently with a cyanine fluorophore. As shown in Figure 2C, **8** and IRDye-800CW, but not **9** and FNIR-774, show dramatic labeling. Consistent with the notion that these fluorescent bands result from heptamethine cyanine labeling, no signal was observed in the 700 nm emission channel. These studies provide the first evidence that C4-phenol-substituted cyanines can react with cellular proteins, presumably via the S-alkylation pathway described above. Additional studies will be required to determine if covalent modification, which is likely undesirable for an imaging modality, occurs during *in vivo* imaging applications. Guided by the studies above, we chose to examine **9**, now termed Ureter Label-766 (UL-766), *in vivo*.

We compared the bio-distribution and clearance of IRDye-800CW, which has been studied previously for ureter imaging,¹⁰ and UL-766. The two compounds were injected intravenously (0.09-mg/kg) into rats and we monitored the behavior of injected NIR fluorophores in real-time over 60 min. Details of the imaging studies are described in the supporting information. As shown in Figure 3, IRDye-800CW exhibits a complex bio-distribution, being mostly found in the bile duct, intestine, and kidney. Much to our delight, UL-766 demonstrated nearly exclusive renal clearance, with no visible nonspecific background signal in any organs other than the kidney or ureter. To quantify these differences, we measured the Contrast-Background-Ratio (CBR) of the kidney over time with both IRDye-800CW and UL-766. Based on these curves, the CBR is typically over 2 \times higher for UL-766 than for IRDye-800CW. Moreover, the time window for ureter visualization is longer and starts nearly immediately after injection of UL-766.

The ureter is vulnerable to iatrogenic injuries during various surgical procedures. This is largely attributed to the hidden position of the ureter in the retroperitoneum, combined with

their elongated course along virtually every level of the retroperitoneum and upper pelvis. The visualization of the ureter without inserting additional stents or evoking peristalsis by touching instruments would be beneficial to check for acute ureteral injuries resulted from external trauma, open surgery, laparoscopy, and endoscopic procedures. Ureteral leakage could also be instantaneously examined after ureteral anastomosis was performed.

This study details a new fluorophore, UL-766, with promising features for ureter visualization. UL-766 undergoes highly selective and rapid renal clearance and can be used to display the ureter using a NIR fluorescence imaging system. UL-766 exhibits improved specificity for renal clearance compared to the commercially available IRDye-800CW dye. The compound can be injected intravenously at a low dose, and is sensitive enough to visualize over an extended period of time. Moreover, this compound exhibits reduced reactivity with biological nucleophiles. The reduced reactivity of UL-766 and related molecules could be important from a clinical toxicology perspective. However, it is likely that the degree to which compounds are subject to undesirable modification is highly dependent on their clearance rates and the context in which they are used (i.e. if they are targeted or not). Further efforts along these lines is likely merited. The favorable properties of UL-766 make it a promising candidate for clinical use, and further studies towards this goal are currently underway.

Supplementary Material

Refer to Web version on PubMed Central for supplementary material.

Acknowledgment

We thank Dr. Joseph Barchi, NCI-CCR, for NMR assistance and Dr. James Kelley, NCI-CCR, for mass spectrometric analysis. The authors also thank to Dr. George Zalzal and ENT department at CNHS for generous gift for operating microscope. This work was supported by the Intramural Research Program of the National Institutes of Health, National Cancer Institute, Center for Cancer Research and the Sheikh Zayed Institute for Pediatric Surgical Innovation. Dr. Luke Lavis, Janelia Research Campus, Howard Hughes Medical Institute, is thanked for assistance with quantum yield determination.

References

1. Perrin DP, Vasilyev NV, Novotny P, et al. Image guided surgical interventions. *Curr Probl Surg* 2009;46: 730–766. [PubMed: 19651287]
2. Nguyen QT, Tsien RY. Fluorescence-guided surgery with live molecular navigation--a new cutting edge. *Nature reviews Cancer*. 2013;13: 653–662. [PubMed: 23924645]
3. Garland M, Yim JJ, Bogyo M. A Bright Future for Precision Medicine: Advances in Fluorescent Chemical Probe Design and Their Clinical Application. *Cell Chem Biol* 2016;23: 122–136. [PubMed: 26933740]
4. Rosenthal EL, Warram JM, Bland KI, Zinn KR. The status of contemporary image-guided modalities in oncologic surgery. *Ann Surg* 2015;261: 46–55. [PubMed: 25599326]
5. Martinic I, Eliseeva SV, Petoud S. Near-infrared emitting probes for biological imaging: Organic fluorophores, quantum dots, fluorescent proteins, lanthanide(III) complexes and nanomaterials. *J Lumin* 2017;189: 19–43.
6. Gioux S, Choi HS, Frangioni JV. Image-Guided Surgery Using Invisible Near-Infrared Light: Fundamentals of Clinical Translation. *Mol Imaging*. 2010;9: 237–255. [PubMed: 20868625]

7. Reinhart MB, Huntington CR, Blair LJ, Heniford BT, Augenstein VA. Indocyanine Green: Historical Context, Current Applications, and Future Considerations. *Surgical innovation*. 2015;23:166–175. [PubMed: 26359355]
8. Verbeek FPR, van der Vorst JR, Schaafsma BE, et al. Intraoperative Near Infrared Fluorescence Guided Identification of the Ureters Using Low Dose Methylene Blue: A First in Human Experience. *J Urology*. 2013;190: 574–579.
9. Matsui A, Tanaka E, Choi HS, et al. Real-time, near-infrared, fluorescence-guided identification of the ureters using methylene blue. *Surgery*. 2010;148: 78–86. [PubMed: 20117811]
10. Korb ML, Huh WK, Boone JD, et al. Laparoscopic Fluorescent Visualization of the Ureter With Intravenous IRDye800CW. *J Minim Invas Gyn* 2015;22: 799–806.
11. Gorka AP, Nani RR, Schnermann MJ. Cyanine polyene reactivity: scope and biomedical applications. *Org Biomol Chem* 2015;13: 7584–7598. [PubMed: 26052876]
12. Luo SL, Zhang EL, Su YP, Cheng TM, Shi CM. A review of NIR dyes in cancer targeting and imaging. *Biomaterials*. 2011;32: 7127–7138. [PubMed: 21724249]
13. Strekowski L, Lipowska M, Patonay G. Substitution-Reactions of a Nucleofugal Group in Heptamethine Cyanine Dyes - Synthesis of an Isothiocyanato Derivative for Labeling of Proteins with a near-Infrared Chromophore. *J Org Chem* 1992;57: 4578–4580.
14. Mujumdar SR, Mujumdar RB, Grant CM, Waggoner AS. Cyanine-labeling reagents: Sulfobenzindocyanine succinimidyl esters. *Bioconjugate Chem* 1996;7: 356–362.
15. Nani RR, Shaum JB, Gorka AP, Schnermann MJ. Electrophile-Integrating Smiles Rearrangement Provides Previously Inaccessible C4'-O-Alkyl Heptamethine Cyanine Fluorophores. *Organic Letters*. 2015; 17: 302–305. [PubMed: 25562683]
16. Sato K, Gorka AP, Nagaya T, et al. Role of Fluorophore Charge on the In Vivo Optical Imaging Properties of Near-Infrared Cyanine Dye/Monoclonal Antibody Conjugates. *Bioconjug Chem* 2016;27:404–413. [PubMed: 26444497]
17. Sato K, Gorka AP, Nagaya T, et al. Effect of charge localization on the in vivo optical imaging properties of near-infrared cyanine dye/monoclonal antibody conjugates. *Mol Biosyst* 2016;12: 3046–3056. [PubMed: 27452807]
18. Sato K, Nagaya T, Nakamura Y, et al. Impact of C4'-O-Alkyl Linker on in Vivo Pharmacokinetics of Near-Infrared Cyanine/Monoclonal Antibody Conjugates. *Mol Pharm* 2015;12: 3303–3311. [PubMed: 26261913]
19. Choi HS, Nasr K, Alyabyev S, et al. Synthesis and In Vivo Fate of Zwitterionic Near-Infrared Fluorophores. *Angew Chem Int Edit*. 2011;50: 6258–6263.
20. Choi HS, Gibbs SL, Lee JH, et al. Targeted zwitterionic near-infrared fluorophores for improved optical imaging. *Nat Biotechnol* 2013; 31: 148–153. [PubMed: 23292608]
21. Harmatys KM, Cole EL, Smith BD. In vivo imaging of bone using a deep-red fluorescent molecular probe bearing multiple iminodiacetate groups. *Mol Pharm* 2013; 10: 4263–4271. [PubMed: 24099089]
22. Nani RR, Gorka AP, Nagaya T, et al. In Vivo Activation of Duocarmycin-Antibody Conjugates by Near-Infrared Light. *ACS Central Sci* 2017;3: 329–337.
23. Levitus M, Ranjit S. Cyanine dyes in biophysical research: the photophysics of polymethine fluorescent dyes in biomolecular environments. *Q Rev Biophys* 2011;44: 123–151. [PubMed: 21108866]
24. Zaheer A, Wheat TE, Frangioni JV. IRDye78 conjugates for near-infrared fluorescence imaging. *Mol Imaging*. 2002;1: 354–364. [PubMed: 12926231]
25. Lee H, Mason JC, Achilefu S. Heptamethine cyanine dyes with a robust C-C bond at the central position of the chromophore. *J Org Chem* 2006;71: 7862–7865. [PubMed: 16995699]

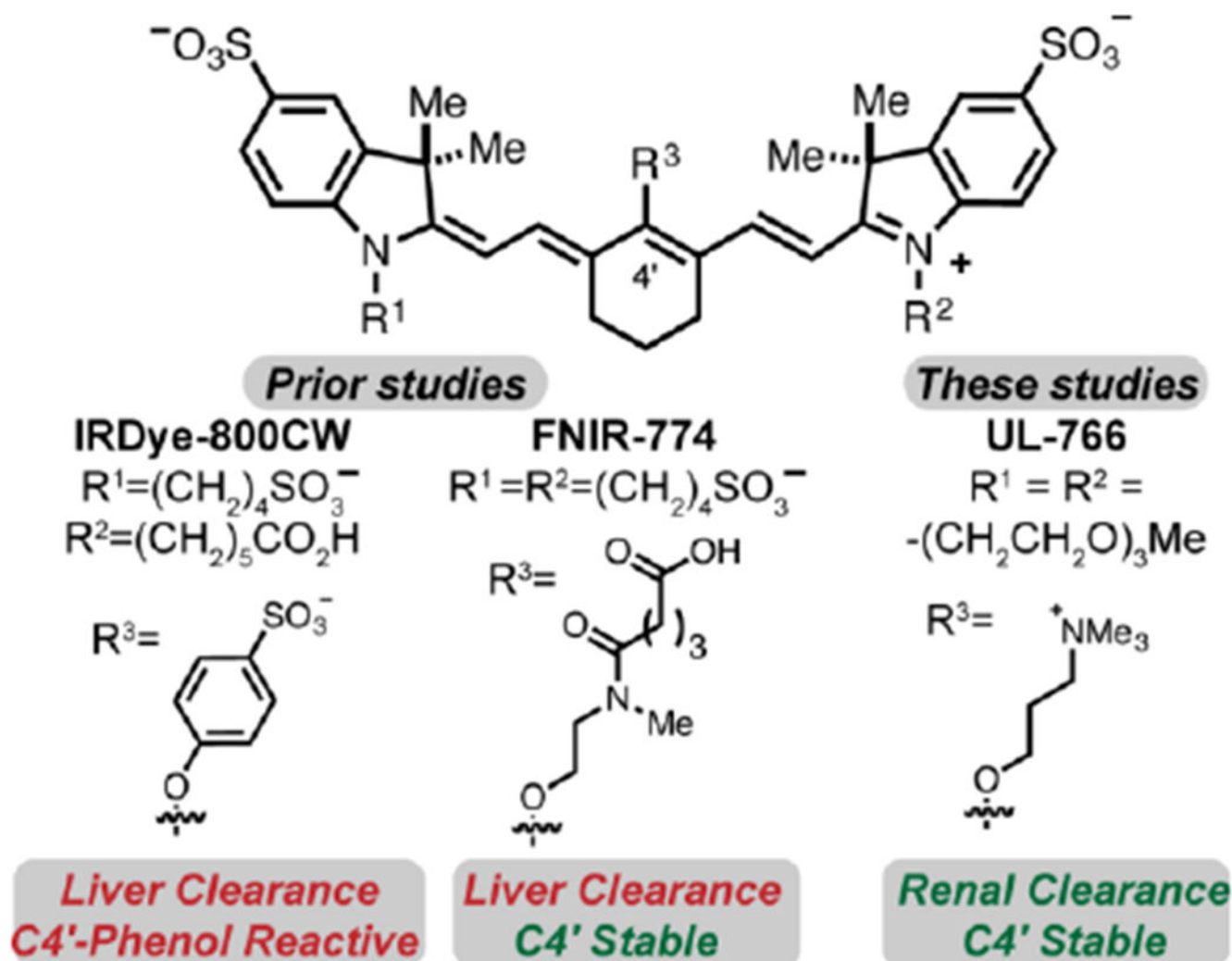
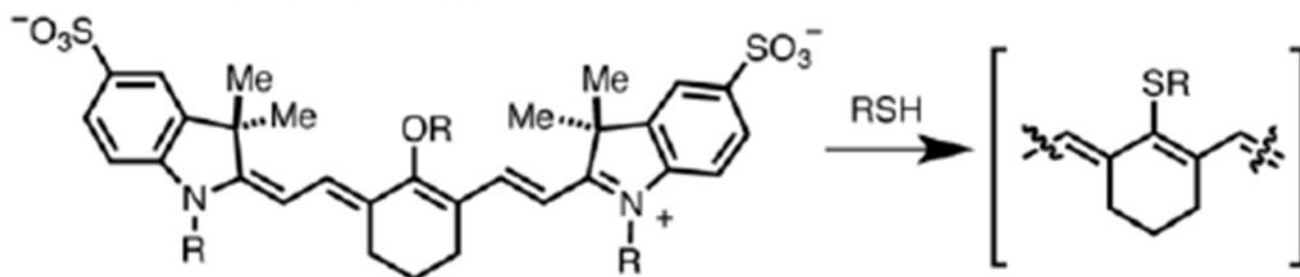


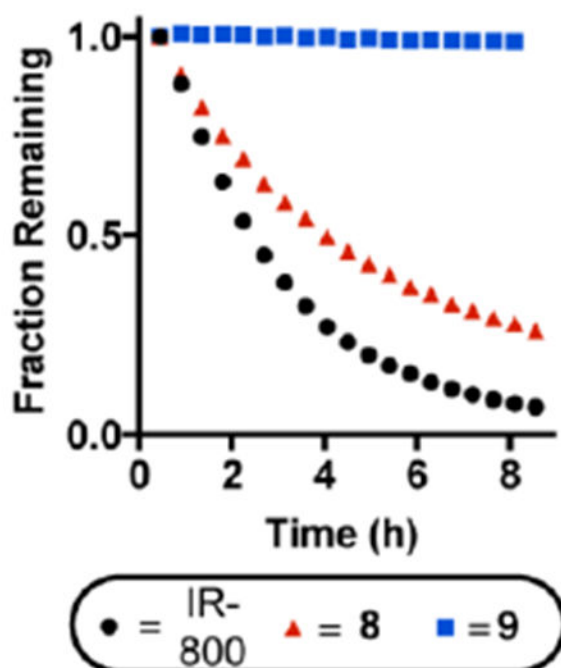
Fig 1.

Key prior cyanines, IRDye-800CW and FNIR-774, and the compound reported here, UL-766.

A. General Reaction



B. Glutathione Addition



C. Proteome Reactivity

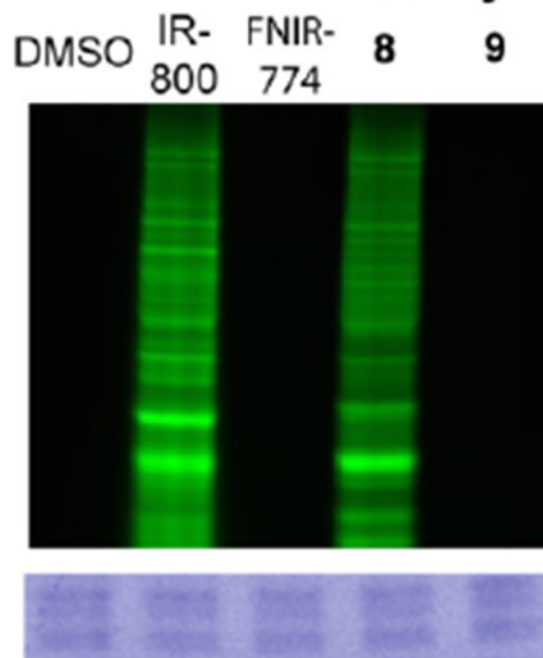


Figure 2:

(A) General reaction manifold for cyanine-thiol adduct formation. (B) Glutathione stability determine by fraction remaining of starting cyanine (10 μ M) in 1 mM GSH in pH 7.4 PBS. (C) Proteome-wide reactivity of cyanines to HEK-293 cells (HEK-293 cell lysate incubated with 10 μ M dye for 24 h and run on an SDS-PAGE gel). The green signal is emission using 800 nm excitation and the blue signal is Coomassie staining to confirm protein loading.

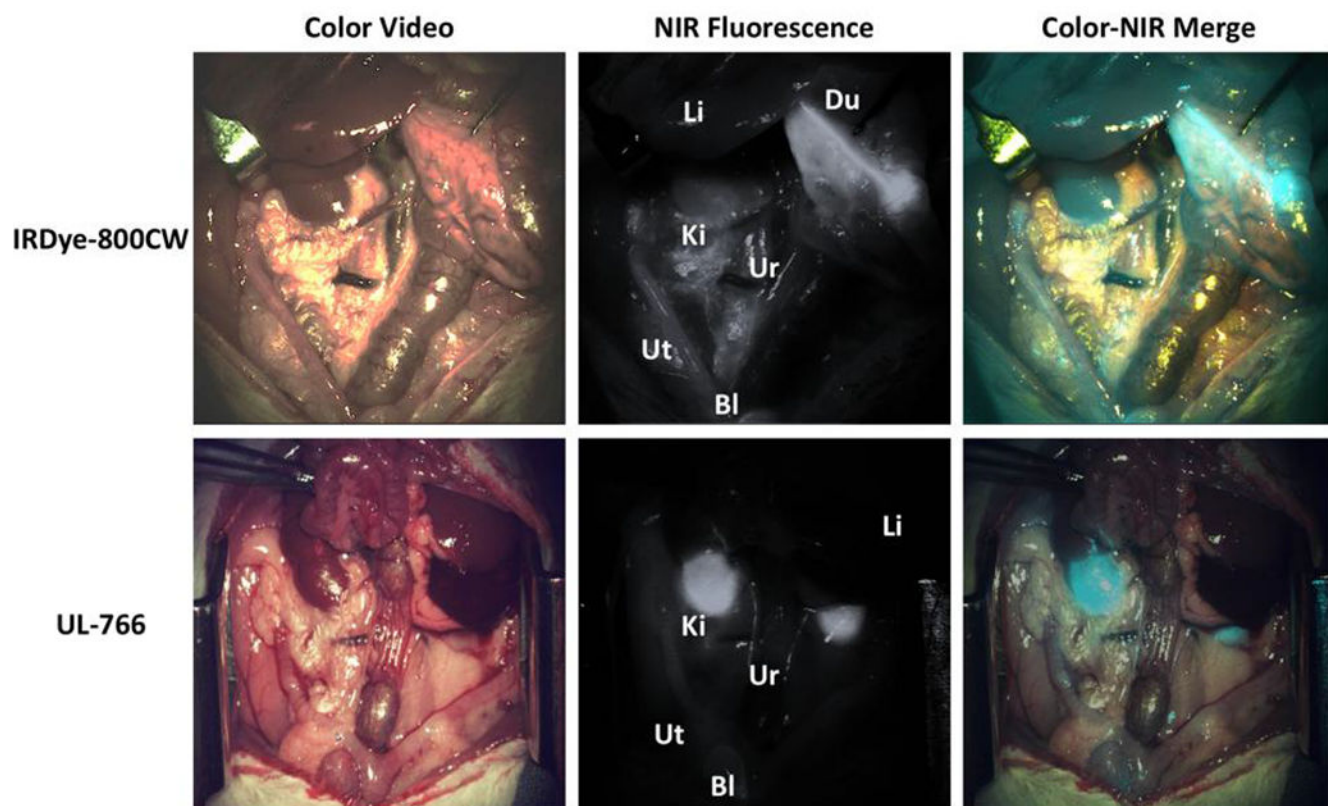


Fig 3. NIR fluorescence-guided intraoperative identification of the ureter. Shown are the color video (left column), NIR fluorescence (middle column), and a pseudo-colored (Cyan) merged image of the 2 (right column). Exposure time was 33 ms for all NIR fluorescence images. Li:liver, Du:Duodenum, Ki:kidney, Ur: ureter, Ut: uterine, Bl: Bladder.

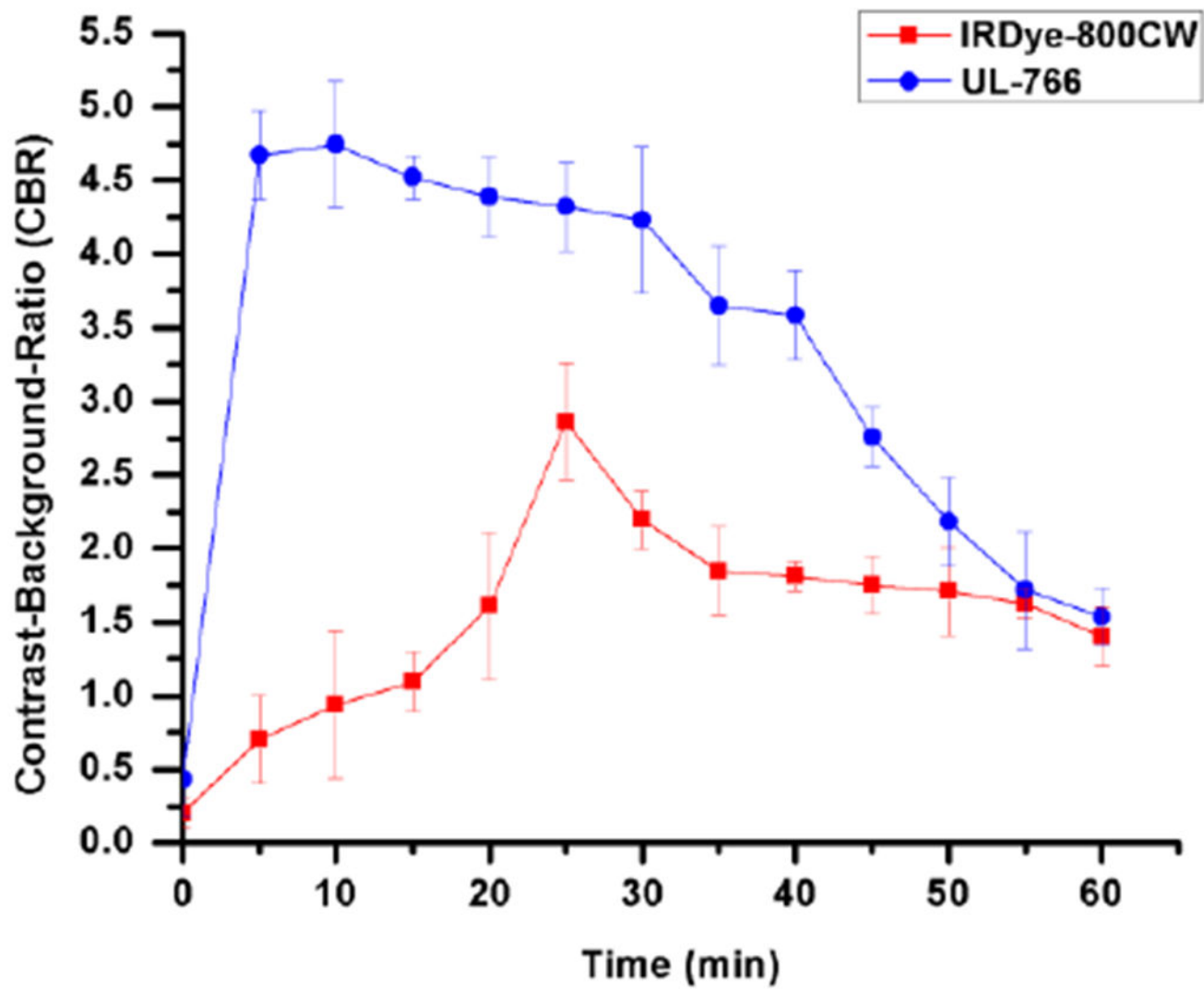
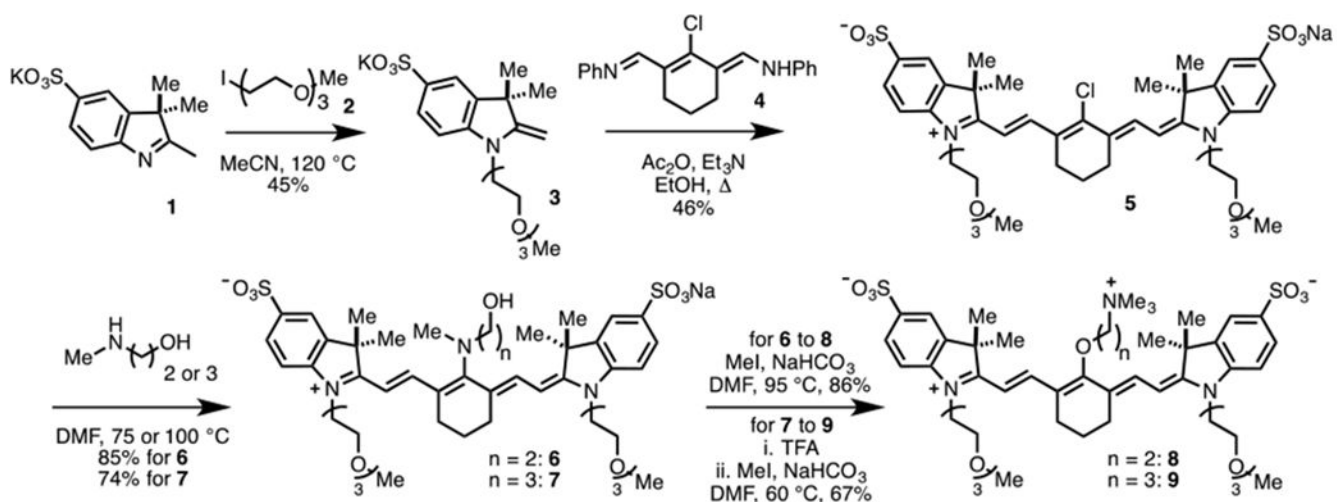


Fig 4. Contrast-to-background ratio of kidney in rats (n = 4). Bars represent mean \pm SEM.



Scheme 1.
Synthesis of **8** and **9**.

Table 1Key spectroscopic properties of FNIR-774, **8**, and **9** (all measured in pH 7.4 PBS).

	λ_{\max} (nm)	ϵ ($M^{-1}cm^{-1}$)	λ_{em} (nm)	Φ_F	brightness ($\epsilon \times \Phi_F$)
FNIR-774	774	204,000	789	0.10	21,000
8	774	255,000	796	0.067	17,000
9	766	229,000	789	0.095	22,000

Author Manuscript

Author Manuscript

Author Manuscript

Author Manuscript